The role of molecular mobility in the yielding of solid polymers

J. M. Lefebvre* and B. Escaig
Université des Sciences et Technologies de Lille/CNRS, Laboratoire Structure et Propriétés de l'Etat Solide, 59655 Villeneuve d'Ascq, France
(Received 28 January 1992; revised 24 June 1992)

The yielding behaviour of various thermoplastics and thermosets is reviewed in terms of a thermally activated dislocation propagation mechanism. The activation parameters are related to the local polymer structure (entanglement topology, chain flexibility) and to its molecular dynamics reflected in the secondary relaxation processes.

(Keywords: yielding; thermoplastics; thermosets; chain flexibility; molecular mobilities)

INTRODUCTION

It is generally accepted that the temperature range of useful ductile behaviour of engineering plastics spreads from glass transition temperature, T_g, down to secondary transition temperatures, mostly T_β but sometimes also T_γ.

An understanding of the mechanical importance of these temperatures obviously requires a comprehensive knowledge of the effect of molecular mobility on mechanical behaviour. What are the specific influences of molecular mobility on properties such as ageing, impact, yielding, creep, fatigue and their temperature dependences? What is the relative importance of polymeric molecular structure: amorphous, semicrystalline, thermoset with respect to such local mobility? Such an understanding has not yet been achieved, and to do so, a plastic deformation model at the molecular scale is needed.

We proposed a model of this type some years ago[1–3]. Using a metallurgical approach, we assume that plastic deformation in solid polymers occurs by nucleation and growth of Somigliana dislocation loops, i.e. microshear band discs, in the molecular arrangement of the amorphous phase. Clearly, this refers to conditions where crazing is not favoured and where deformation is limited to yielding. Thermally activated deformation can then be modelled as a dislocation propagation mechanism, and the role of secondary transition processes can be investigated. Since the first studies on simple amorphous polymers like atactic polystyrene (PS) and poly(methyl methacrylate) (PMMA)[4], further experimental results have been obtained on other polymer families, like semicrystalline polypropylene (PP) and related blends[5], model epoxides with controlled cross-linking and flexibility[6] and unsaturated polyesters of various flexibilities[7]. The aim of this paper is to discuss how the original model compares with experiment, and to learn from this the specific behaviours controlled by molecular mobility in the plastic deformation of solid polymers.

First, it is useful to recall the thermodynamic characteristics of polymers as compared to atomic solids. Due to their chain structure, many more degrees of freedom can be activated by temperature. As a result, not only are several transition temperatures found (T_g, T_β, T_γ etc.) instead of just one (0.5 T_m, T_m is the melting point), but the molar specific heat of the monomer unit, and therefore its molar entropy, are much higher than for simple solids, which results in larger activation entropies during processes. Finally, great emphasis has to be put on entropy effects. The mechanical importance of entropy effects in polymers is a strong distinctive feature from the case of atomic solids in metallurgical analysis, and their effect on properties will be demonstrated below.

A review of the proposed plastic deformation model is followed by discussion of the experimental relevance of its main features through various polymer systems, that is, the frequency of the elementary deformation event, ν_{def}, the internal stress, σ_i, and the activation parameters: activation volume, V_a, effective stress σ^*, activation free energy ΔG_a and athermal temperature T_a.

THE PROCESS OF YIELDING REVISITED

On the basis of arguments given in previous papers[1–3] the non-elastic deformation of a glassy polymer is modelled by the nucleation and growth of localized slip nuclei, or microshear band discs, i.e. Somigliana dislocation loops. The flow kinetics follows from the macroscopic (non-elastic) strain rate, $\dot{\varepsilon}_p$, produced by the statistical development of critical shear nuclei, and is estimated from simple kinetic arguments[8,9]:

$$\dot{\varepsilon}_p = N\varepsilon_0 \nu_{def} = (N/V_{tot})V_0 \nu_{def} \quad (1)$$

where N is the number of active sites where nuclei may grow in the total volume V_{tot}, ε_0 is the average strain achieved by each successful activation event, V_0 is the fully expanded nucleus volume and ν_{def} is the activation rate, i.e. the fraction of the large number of starting nuclei that achieves expansion per unit time. Now ε_0 is a volume

* To whom correspondence should be addressed

0032-3861/93/030518-10

average, so that $\varepsilon_0 \cong e_0(V_0/V_{tot})$ with $e_0 \cong 1$, from which equation (1) follows.

It is worth noting that, in contrast with usual atomic crystals, no 'Frank network', i.e. pre-existing dislocation network, exists. Instead, the basic 'as-grown' heterogeneity, from which the strain localization is derived, comes from the glass structure itself, where it is plausible that shear nuclei occur when steric hindrances at each level of stress are weaker than elsewhere. This results in the nucleation defect density, N/V_{tot}, which is more commonly expressed as a linear defect (or dislocation) density $\rho_0 = NL_0/V_{tot}$, given the defect strength b (the Burgers vector length) so that $V_0 = bS_0$ and the defect contour length $L_0 = 2(\pi S_0)^{1/2}$ assuming a circular shape. Accordingly, equation (1) can be rewritten as:

$$\dot{\varepsilon}_p/v_{def} = (bV_0/4\pi)^{1/2}\rho_0 \qquad (1')$$

Since v_{def} can be determined at $\dot{\varepsilon}_p$ by experiment (see below), arbitrarily taking $V_0 \cong 2V_a$ (where V_a is the experimentally known activation volume) and b as the mean chain radius ($v = a\pi b^2$, where v is the monomer unit volume and a is the unit length along the chain), an order of magnitude of ρ_0 can be obtained. *Table 1* gives ρ_0 values at yield and at low temperature ($T \cong 200$ K) for the various polymer systems investigated. As expected, for strongly cross-linked resins ρ_0 lies in the lowest range, while for thermoplastics it is higher, at a level quite comparable to yield in crystals (10^7 cm^{-2}). A rather low value of ρ_0 is found for semicrystalline PP systems: dislocation-like defects are assumed to be developed there in the intercrystal amorphous phase which should be relatively entangled, giving rise to an intermediate nucleation density.

Another parameter in the model is the so-called internal stress, σ_i, which is the back stress resulting from the molecular misfit left behind in the wake of developing dislocations in a glassy phase. Due to the non-periodic distribution of molecular sites over the slip interface, the relative shift of one of its lips relative to the other by a given vector $\langle b \rangle$ creates a number of molecular misfits, i.e. a stacking fault interface of energy per unit area, γ, is trailed behind the moving dislocation. This back stress is defined as:

$$\sigma_i = \gamma/\langle b \rangle \qquad (2)$$

Table 1 Values of macroscopic strain rate ($\dot{\varepsilon}_p$), activation rate (v_{def}), defect strength, Burgers vector of shear shift (b) (for DGEBA resin, b is taken as for PC; for DGEBU resin, b is taken as for PET; for DEG unsaturated polyester, b is taken as for PS due to lateral phenyl rings in styrene links), fully expanded nucleus volume (V_0) and nucleation defect density (ρ_0)

Polymer	$\dot{\varepsilon}_p$ (s^{-1})	v_{def} (Hz)	b (Å)	V_0 (Å^3)	ρ_0 (10^5 cm^{-2})	Ref.
PS	10^{-4}	10^3	4.8	1800	380	4
PMMA	3×10^{-5}		4.6	440	240	4
PP and blends	4.5×10^{-5}	85×10^3	3.5	1000	3	5, 15
DEG-polyester	7.6×10^{-5}	10^6	4.8	400	0.6	7
DGEBU-DDM	4.5×10^{-5}	0.5×10^6	2.8	140	1.6	6
DGEBA-DDM	4.5×10^{-5}	2×10^6	3.2	340	0.2	6
DGEBA-HMDA	4.5×10^{-5}	2×10^6	3.2	240	0.3	6

where γ is an interface energy, i.e. a non-local parameter in the sense that it depends on intermolecular configurations more or less repeated throughout the whole interface. During the pre-yield stage, it is plausible that shear loops are formed within more densely packed regions of the glass as the applied stress and the non-elastic strain increase, so that γ (and σ_i) is an increasing function of this strain. At yield, γ has reached a steady value that can be approximated by an elastic argument due to Friedel[10] as $\mu\langle b \rangle/100$ in order of magnitude, where μ is the shear modulus, so that σ_i/μ should be temperature independent and of the order of 10^{-2}. Experimental measurements agree with this estimation, ranging from 0.8×10^{-2} in PS, 1.3×10^{-2} in PMMA[4], 1.7×10^{-2} in PP and its blends[5], to a little more in thermoset resins, $\sim 3.5 \times 10^{-2}$, as found for the model epoxies investigated below[6] (all these figures relate to shear modulus values taken at the deformation frequency v_{def} given in *Table 1*).

Up to now, we have modelled the plastic flow of a nearly glassy phase, with no consideration of its polymeric nature. The latter is introduced by taking into account chain entanglements, or chain cross-links, which should act as local obstacles to developing shear-band loops, at the origin of a strong thermal dependence of the flow stress. In the thermal activation formalism, the flow stress is written as[8,9]:

$$\sigma_a = \sigma_i + \sigma^*(T, \dot{\varepsilon}) \qquad (3)$$

where σ_i/μ is taken as temperature independent, in contrast to σ^*/μ; $\sigma^* = \sigma_a - \sigma_i$ is termed the effective stress, or the thermal component of the flow stress. Thus, entanglements are viewed as local barriers to be overcome with the help of thermal fluctuations; these barriers are characterized by the usual activation parameters: ΔG_a, the activation free energy, V_a the activation volume, or spatial extension of the barrier, and the activation entropy ΔS_a. All these parameters can be deduced from experiment[8,9]. Of particular interest is the 'athermal' temperature, T_a related to the barrier energy ΔG_0 by:

$$\Delta G_0 = \alpha k T_a \qquad \alpha = \ln(\dot{\varepsilon}_0/\dot{\varepsilon}_p) \qquad (4)$$

This refers to the Arrhenius constitutive equation for the non-elastic strain rate, $\dot{\varepsilon}_p = \dot{\varepsilon}_0 \exp -(\Delta G_a/kT)$, which can be inverted as $\Delta G_a = \alpha kT$ with $\alpha = \ln(\dot{\varepsilon}_0/\dot{\varepsilon}_p)$. Thus in a constant strain rate test, ΔG_a at yield is proportional to temperature. Moreover the barrier is overcome by the thermal energy ΔG_a and by the mechanical work, $(\sigma_a - \sigma_i)V_a$, hence[8,9]:

$$\Delta G_0 = \Delta G_a + \sigma^* V_a \qquad (5)$$

At temperature T_a, $\sigma^* = 0$ (or $\sigma_a = \sigma_i$), so that $\Delta G_0 = \Delta G_a = \alpha k T_a$: the barrier can then be considered as being 'transparent' to thermal activation, in the sense that thermal fluctuations are strong enough to overcome it without any mechanical aid. Therefore T_a, which can be easily determined by stress relaxation experiments[8,9,11], is a direct measure of the barrier height ΔG_0.

These activation parameters have been modelled within the frame of dislocation theory[1-3]. Entanglements are zones of local steric hindrances where relative movements of chain units are strongly restricted. These zones should cause very bad molecular misfits when swept out by a shear band of mean shift $\langle b \rangle$, unless entanglement points are first diffused away, off the slip interface, by a few molecular spacings. This process can

be viewed as nucleating an additional dislocation loop of Burgers vector, $\beta = b(M) - \langle b \rangle$, where the local Burgers vector $b(M)$ fitting the molecular arrangement in zone M differs too much from the mean shift $\langle b \rangle$. Of course the β-loop is here prismatic, i.e. the β vector does not lie on the glide interface defined by $\langle b \rangle$ and the main dislocation line (or shear-band front). β should be much smaller than $\langle b \rangle$; it should be close to the fluctuations of atomic spacings. The respective magnitudes of both $\langle b \rangle$ and β may be estimated from electronic radial distribution functions (r.d.f.) derived from X-ray data. $\langle b \rangle$ corresponds to the average distance of closest approach of two chains, whereas the peak width of the r.d.f. curves provides a measure of this fluctuation in atomic spacings[1]; i.e. for β: it gives $\beta \cong 1$ Å as compared to $\langle b \rangle \cong 5$ Å for vinyl chains like PS or PMMA[12]. Summarizing, the overall picture of a Somigliana dislocation in polymers should consist of two components: (i) a stacking fault of shear shift $\langle b \rangle$ where molecular misfits are weaker, and (ii) a collection of localized loops of vector β, where entanglements cut through the fault. Propagating such dislocations through the polymer thus requires a shear stress, σ_a, equal to the back stress of the stacking fault component, σ_i, plus the thermal component stress σ^* needed to overcome the entanglement zones, i.e. to nucleate the β loops right at the edge of the main dislocation line and merging with it. This process describes how the Burgers vector of the Somigliana dislocation is varied continuously along the line as $\langle b \rangle \pm \beta$.

Two parameters are needed to describe the entanglement obstacles: (i) the radius δ of the zone within which the slipping of units one above the other is restricted; and (ii) the spacing λ of entanglements in the slip interface, which is related to their three-dimensional spacing, x, by the relation[3]:

$$2\delta\lambda^2 = x^3 = M_e/(\rho N_A) \tag{6}$$

where $M_e = N_e m$, the molecular weight found along the chain between entanglements, ρ is the specific weight of the polymer and N_A is Avogadro's number. The radius δ obviously depends on the chain stiffness, a characteristic of the chain structure; it is proposed to take $\delta \cong s \cong 2l$, where s is the length of the statistical chain element[1-3], i.e. twice the persistence length l, and is known from small angle neutron or X-ray scattering data[13]. *Table 2* gives values of l, $s = \delta$, M_e and x for vinyl chains PS, PMMA and PP.

It has been shown[3] that two cases can be distinguished.

1. For polymers for which $x > 0.93\delta$, the obstacles act independently of each other; the activation volume is then proportional to s^2 (i.e. is scaled by the square of the persistence length) as:

$$V_a \cong f\beta s^2 \tag{7}$$

where f is a polymer-independent but slightly stress-dependent factor, of the order of unity and smaller than π. *Table 2* shows that for vinyl thermoplastics, which fall in this group, experiment agrees reasonably with the theory. It is also noticed that the extra-matter associated with the non-conservative β loops reduces to only one to three unit links, since $\langle \beta A \rangle$ (A is the area of β loop) averaged over all possible β orientations gives about $\langle \beta A \rangle \cong 0.6\beta A = 0.6 V_a$. This result is reasonable in view of the necessary removal of the entanglement point from the slip interface.

2. For strongly cross-linked polymers, for which $x < 0.93\delta$, the chain rigidity makes obstacles overlap each other, so that Burgers vector fluctuations are now required all along the moving dislocation line, entailing continuous fluctuations in its core energy. This case is akin to the Peierls forces mechanism in some crystalline solids, frequently observed in organic solids where steric hindrances prevail[14], like α-sulphur, or b.c.c. hexamine. Dislocation motion should then arise through the well-known (β) double-kink model, resulting in a clearly stress-dependent activation volume as:

$$V_a \cong f'\beta\langle b \rangle^2(\sigma(0) - \sigma_i)/(\sigma_a - \sigma_i) \tag{8}$$

where $\sigma(0)$ is the yield stress at 0 K, $\langle b \rangle$ is a mean chain radius and f' is a constant factor (except for temperatures near 0 K at which $f' = 0$). Unsaturated polyesters, on which experimental results are reported below, may be an example of this case.

EXPERIMENTAL COMPARISONS AND DISCUSSION

Before reviewing the different points of comparison of the above yielding model with experiment, it is necessary to give a brief description of the polymer systems that have been investigated; further details are available in refs 5–7 and 15.

Table 2 Values of specific weight of polymer (ρ), molecular weight along chain between entanglements (M_e), persistence length (l) (taken as $0.5a(1 + C_\infty)$ for PP, with a = unit length along chain and C_∞ = usual chain parameter, $C_\infty = \langle r^2 \rangle / N_a^2$), radius of zones within which slip of units is restricted around an entanglement point (δ), three-dimensional spacing of entanglements (x), low temperature activation volume (V_a)

Polymer	ρ (g cm^{-3})	M_e (g mol^{-1})	l (Å)	$\delta = s$ (Å)	x (Å)	V_a (Å^3)	V_a/δ^2 (Å)	$\sigma_i(T_a)$ exp (MPa)	$\mu\langle b \rangle/10x$ (MPa)
Atactic PS	1.06	19000	11[a]	22	31	900[b]	1.86	20	18
Atactic PMMA	1.19	9150	5.5[a]	11	23	220[b]	1.82	25	24
Isotactic PP	0.86	3500	8	16	19	500[c]	1.96	11.5[d]	12

[a] Ref. 13
[b] Ref. 4
[c] Refs 5 and 15
[d] Ref. 5

Materials

Three polymer systems were investigated by performing compressive deformation tests at a constant strain rate of the order of $10^{-5}\,s^{-1}$ (see *Table 1*) and in a temperature range of 77–400 K.

Pure PP homopolymer was compared to its rubber-modified blend PP/high density polyethylene (HDPE)/ethylene propylene rubber (EPR), with 3.5 wt% HDPE and 17.5 wt% EPR, a random ethylene propylene copolymer. SEM and TEM observations show core–shell particles in the micrometre range. Observation of mechanical loss peaks (1 kHz) shows distinct T_g peaks for EPR (~175 K) and PP (~300 K).

Model epoxies were prepared with the aim of independently varying the molecular flexibility of prepolymer chains, and their degree of cross-linking. Diglycidyl ether of bisphenol A (DGEBA) groups were cross-linked either by an aromatic diamine (DDM) or by an aliphatic one (HMDA); also, more flexible groups of butane diol diglycidyl ether (DGEBU) were cross-linked by DDM. Finally two degrees of cross-linking were achieved for each kind of DGEBA epoxy by using amine blends of monoamine (60%) and diamine (40%): DDM-AN (aniline) for aromatic, and HMDA-HA (hexylamine) for aliphatic hardeners. Chemical formulas of these five epoxies are given in *Table 3*, with their glass transition temperatures obtained by d.s.c. at 20°C min^{-1}. *Table 3* also gives group geometrical dimensions, based on cylindrical beads of length L, radius b (as in *Table 1*), and with a volume taken from Van Krevelen[16] additive

Table 3 Network structure and geometrical dimensions for epoxies

DGEBA-DDM T_g = 448 K

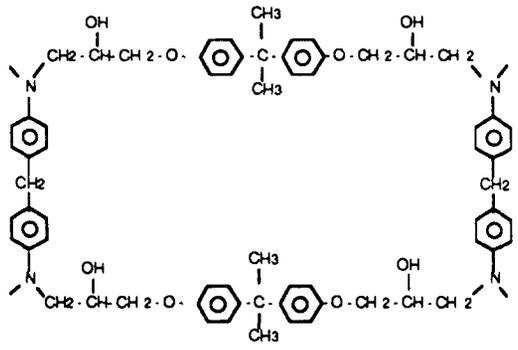

DGEBA-DDM (40%) / AN (60%) T_g = 390 K

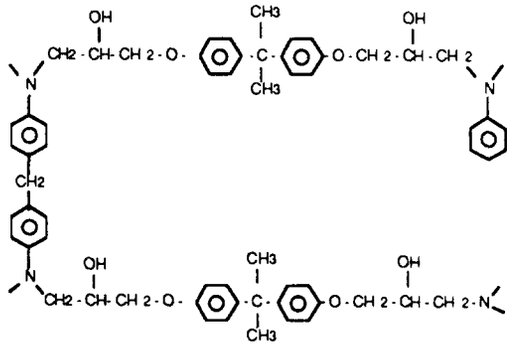

DGEBA-HMDA T_g = 393 K

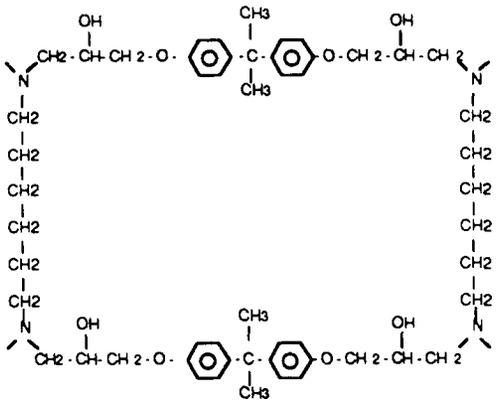

DGEBA-HMDA (40%) / HA (60%) T_g = 338 K

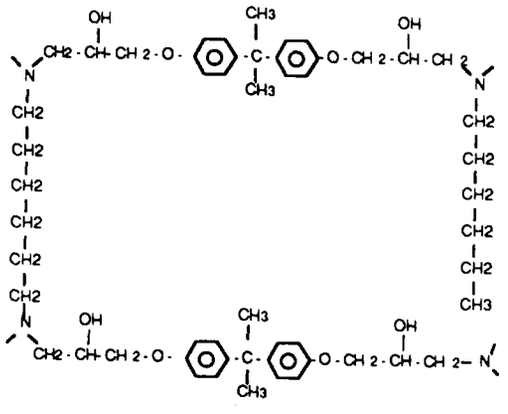

DGEBU-DDM T_g = 345 K

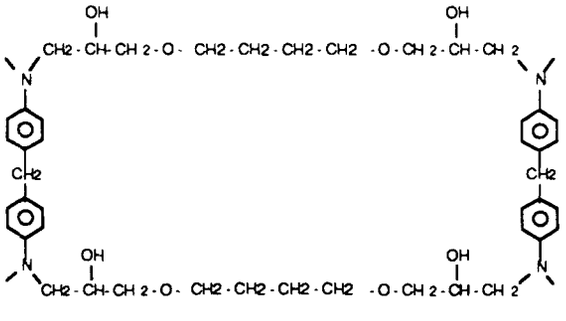

Group	Dimensions		
	Volume (Å^3)	b (Å)	L (Å)
DGEBA	513.5	3.2	16.0
DGEBU	314.2	2.8	12.8
DDM	250.6	2.8	10.2
HMDA	164.7	2.6	7.8

subgroup contributions. Molecular mobilities were characterized by dynamic mechanical analysis (at 7.8 Hz, 500 Hz, and 1.5 MHz)[6] and by ^{13}C solid state n.m.r.[17,18]. It is shown that hydroxyether units, $-CH(OH)-CH_2-O-$, are the mobile entities responsible for the β secondary transition that occurs in all resins in the same temperature range (255–265 K at 500 Hz); the β peak is widely spread over $\sim$100 K, especially as the cross-linking is tighter, but rises from about the same temperature ($\sim$200 K) for any resin[17].

Contrary to the above epoxies, in which the amine N cross-link points have a functionality of three, unsaturated polyesters derived from maleic anhydride (MAA) have cross-link points with a functionality of four, i.e. they are expected to be tighter cross-linked resins, which is actually the case. *Table 4* gives chemical formulas for the two polyesters investigated in this study. They were prepared by reaction of the anhydride on a diol, either propylene glycol (MAA-PG) or diethylene glycol (MAA-DEG), and crosslinked with styrene. Anhydride and diol are equimolar, while the molar ratio R of styrene over MAA is 0.94, corresponding to two styrene units in each link on average, as seen by n.m.r. and shown in *Table 4*. The amount of residual maleate double bonds, $-CH=CH-$ was evaluated by ^{13}C solid state n.m.r.; their concentration is estimated to be 29% in MAA-DEG, and 23% in MAA-PG[18]. Molecular mobilities were characterized by dynamic mechanical analysis (0.1–500 Hz)[7] and by ^{13}C solid state n.m.r.[18]. Both resins show merely a rigid polyester behaviour: apart from glass transition movements (α peak), the only motions occur in styrene links as the rotation of phenyl lateral groups connected with the γ transition (γ peak) is set up; β movements seem to be limited to the chemical groups in the vicinity of the residual unsaturated $-C=C-$ carbons, i.e. to network defects. These defects weaken the network, and may also be at the origin of movements of some $-(CH_2)_2-O-(CH_2)_2-$ ether groups localized nearby in MAA-DEG resins. However, in spite of the expected mobility of such groups, it seems that when in a perfect network region they do not move at all. Finally, PG and DEG resins should have no other β relaxation than that due to network defects (in which case it occurs earlier in DEG). *Table 4* gives group geometrical sizes, computed as in *Table 3*; it shows rather tight networks in which bulky lateral groups, like the phenyl or methyl ones, preclude any local movement of polyester chains.

Table 4 Network structure and geometrical dimensions for unsaturated polyesters

MAA-PG-STY (R = 0.94) Tg = 473K

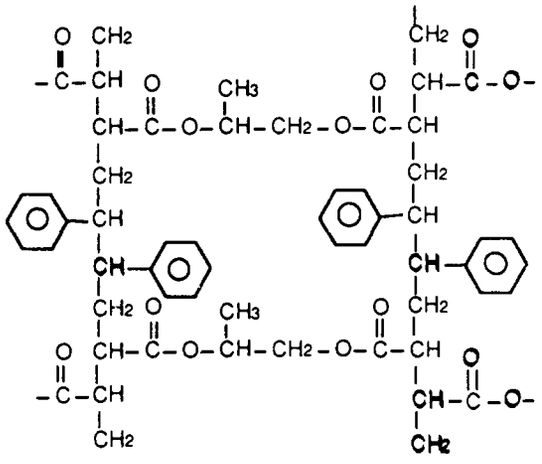

MAA-DEG-STY (R = 0.94) Tg = 378K

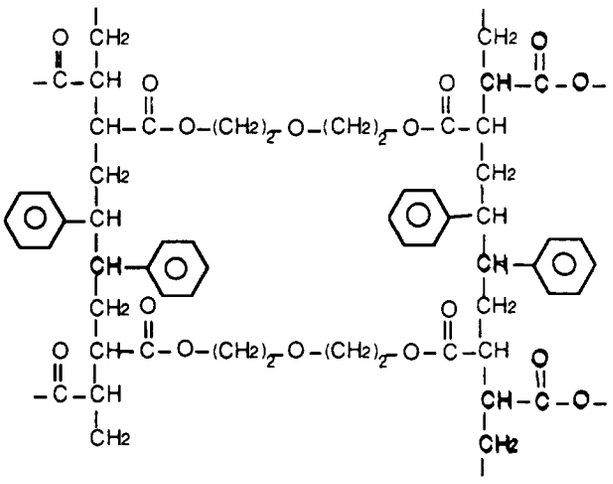

Group	Dimensions		
	Volume (Å^3)	b (Å)	L (Å)
MAA-PG	168.6	3.2	5.2
MAA-DEG	208.8	2.6	9.8
Styrene	336	4.8	4.6

Frequency of elementary activated event in yielding: experimental validity

It is well known that deformation parameters depend on elastic modulus, which depends in turn on frequency, so a problem arises in defining a corresponding frequency for non-elastic (or plastic) behaviour. This frequency should be identified with ν_{def} in equation (1)[8], and an iterative procedure has been defined to deduce it from experiment[19]. It starts from some given frequency, ν_{mod}, at which the elastic modulus value is taken; a curve, $\Delta G_a(T)$, is built up, which is a straight line of slope αk, since $\Delta G_a = \alpha kT$. Since ν_{def} in equation (1) is the activation rate, it should be written as:

$$\nu_{def} = \nu_N \exp - (\Delta G_a/kT) = \nu_N \exp(-\alpha) \qquad (9)$$

where ν_N is an attempt frequency evaluated as $\sim 0.1\nu_D$, ν_D is the Debye frequency of the polymeric solid[8], so that $\nu_N \cong 10^{12}\,s^{-1}$ should hold. Generally the computed value $\nu_{def} = 10^{12}\exp(-\alpha)$ is higher than the starting value ν_{mod}. In such a case, the above procedure is performed with modulus data obtained at a higher frequency and a new deformation frequency ν_{def} is deduced and compared to ν_{mod}. The iteration is performed until $\nu_{mod} \cong \nu_{def}$ is obtained[19]. An illustration of this for PP is given in ref. 15. Values of ν_{def} have been determined by this procedure for some polymer systems and are given in *Table 1* (ranging from 1 kHz to a few megahertz). Finally dislocation nucleation density ρ_0 is deduced from these estimations.

To compare these results to experiment, two examples are given below, which show consistency with other independent measurements. The first is taken from the thermally activated yield observed in PP[5,15]. Equation (5) can be directly checked against experimental data:

ΔG_0, the barrier height, is the reversible work done in overcoming local obstacles; it should not vary noticeably over the stress or temperature range investigated (being expressed in terms of β-loop energy) and can be taken as in equation (4), equal to $\alpha k T_a$; $\Delta G_a = \alpha k T$ and $\sigma^* = \sigma_a - \sigma_i$, so that the quantity $\alpha k T + (\sigma_a - \sigma_i) V_a$ can be compared to $\alpha k T_a$ at any yield condition (T, σ_a). *Figure 1* shows this experimental fit, which is reasonably good given the various experimental scatters: T_a, V_a and $\sigma_i(T_a)$ are obtained independently of the determination of v_{def}, in contrast to $\alpha = 16.3$ and $\sigma_i(T) = \sigma_i(T_a)$ $(\mu(T)/\mu(T_a))$, which are taken at $v_{def} = 85\,\text{kHz} = v_N \exp(-\alpha)$.

The second example is taken from the thermally activated yield observed in polyesters[7]. There, estimation of v_{def} gives 3 MHz for MAA-PG and 1 MHz for MAA-DEG. At 3 MHz, the peak temperatures in MAA-PG are $T_\gamma = 285\,\text{K}$ for γ phenyl rotational movements, and $T_\beta = 455\,\text{K}$ for β movements, probably coupled to α transition movements which already occur in this range due to the overlap of α and β peak widths. Therefore γ movements on one hand, and β–α movements on the other hand can be observed separately at the frequency of elementary deformation events. Now, γ movements should relax the stacking fault energy, probably allowing for a molecular misfit of less energy behind the moving dislocation, thus relaxing σ_i according to equation (2). This σ_i relaxation has been clearly observed in MAA-PG, at 310–320 K, both on the yield stress *versus* T curve, as a small cusp, and on the activation volume *versus* T curve, as a strongly marked cusp shown in *Figure 2a*; this latter effect is explained below. It is significant that although the same behaviour is expected to occur in MAA-DEG, it is not observed on this kind of plot[7]. This is explained when looking at transition temperatures at $v_{def} = 1$ MHz in this polyester network: $T_\gamma \cong 280\,\text{K}$ and $T_\beta = 340\,\text{K}$, which means that γ and β movements are now coupled. Accordingly, at $\sim 300\,\text{K}$, σ_i is already relatively low and the activation volume, which diverges at $T_a = 340\,\text{K} (= T_\beta)$ varies steeply, so that the effect is erased as it occurs. In conclusion, it is seen that only the frequency values determined for the deformation events can explain the behaviour of both polyester resins.

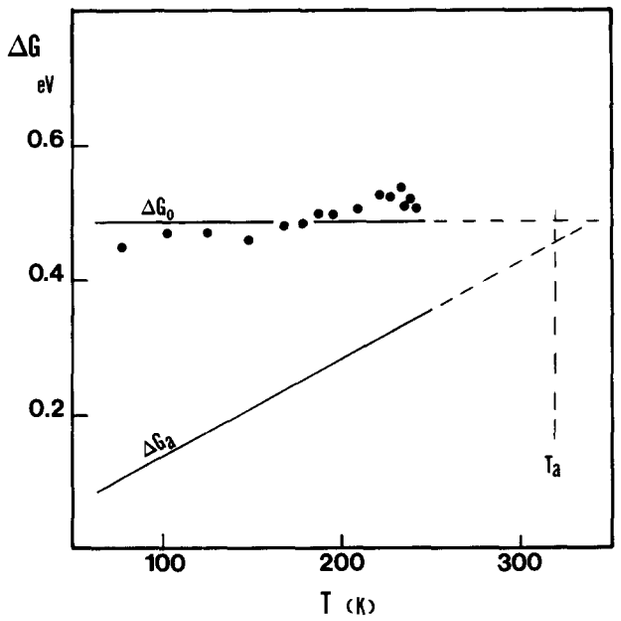

Figure 1 Estimate of the free energy ΔG_0 of the local barrier in PP (after ref. 3)

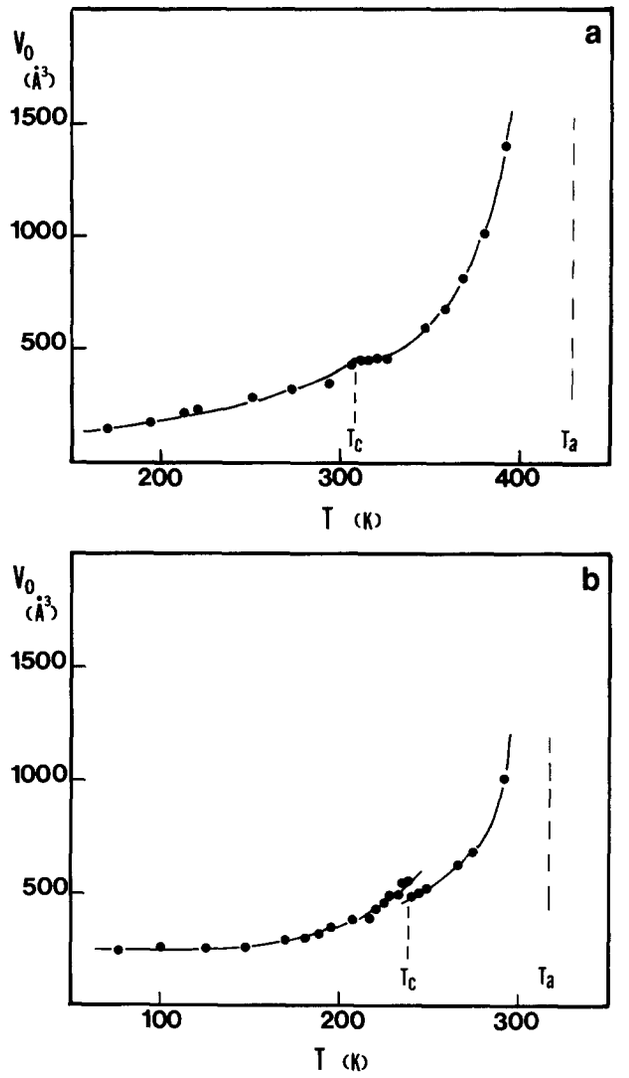

Figure 2 Evolution of the activation volume as a function of temperature for (a) MAA-PG networks and (b) PP

Mechanical influence of molecular mobility

Molecular mobility certainly influences mechanical behaviour. It is of interest to understand how diverse this influence can be on the various yield parameters, the internal stress, σ_i, on the one hand, and the activation parameters, σ^*, V_a, T_a, or ΔG_a, on the other hand. The former depends on non-local, i.e. homogeneous molecular mobilities, those dynamic properties which can be described on any monomer unit in the polymeric phase; it is for this reason that σ_i is not a thermally activated component, i.e. it does not depend on T other than through the elastic modulus μ. The latter depends on local, heterogeneous molecular mobilities, as for example those found at entanglement, or cross-link configurations, that is to say at 'local obstacles'. This basic difference in character is reflected by experimental observations, detailed below.

Internal stress, σ_i. In general, it is expected that σ_i i.e. the stacking fault energy γ in equation (2), should be affected only by molecular motions of sufficient amplitude.

Experimental evidence agrees with this view: these are molecular movements of the glass transition type in PP or PP blends, or rotations of bulky groups of atoms in tightly cross-linked polyester resins which are active on σ_i.

Experimental observation of the activation volume at yield of PP and its blend shows discontinuous drops at characteristic temperatures T_c[5,11] (*Figure 2b*). These temperatures fall at the low temperature side of the glass transition peaks of PP($T_c = 240$ K and 255 K for PP and its blend respectively) and of EPR ($T_c' = 175$ K for the PP blend)[11], so that they coincide each time with the onset of glass-transition-type chain movements. The transition of chains into the rubbery state is expected to entail a drastic drop of σ_i, since the drop in γ energy should parallel that in elastic modulus, since they are proportional. By the same token, σ_i should drop at the start of the modulus drop, and this is observed. In the blend, the first drop at T_c', is due to cancelling of the stacking fault energy as EPR particles are crossed by the developing shear band, while it remains the same across the PP matrix; so this σ_i drop should be weaker, and dependent on EPR concentration. Nevertheless this effect might, for example, favour a concentration of shear bands in regions where the particles are particularly close to one another, which is sometimes observed.

The observed drop in the activation volume, induced by the drop in σ_i has been explained by assuming that near T_c the flow stress, σ_a, is just a little above σ_i (i.e. σ^* is small). Then, the activation kinetics have to take into account both forward and backward jumps of the dislocation over local barriers, resulting in a hyperbolic sine law, $\dot{\varepsilon}_p \sim \sin h(\sigma^* V_a/kT)$, which corresponds to an activation volume $V_a \sim \sigma^{*-1}$. When σ_i drops, σ^* rises so that the usual Arrhenius kinetics, $\dot{\varepsilon}_p \sim \exp -(\sigma^* V_a/kT)$, is resumed while a discontinuous drop is observed in V_a.

A similar effect has been observed in the polyester system described above[7], in which the γ transition is responsible for V_a cusps. Cusps, rather than true drops, are observed, probably because the γ movements, i.e. the rotation of lateral phenyl groups, are less efficient on the stacking fault energy. However, it shows that in tight networks even a γ transition, when it is related to some release of steric hindrances, may have an influence on σ_i.

Finally σ_i merely behaves like μ, the elastic shear modulus. This is well illustrated not only on orders of magnitude ($\sigma_i \cong 10^{-2}\mu$) but, as shown in *Tables 2* and *5*, when experimental figures are compared with an empirical estimate as:

$$\sigma_i = \mu\langle b\rangle/(10x) \quad \text{or} \quad \gamma = \mu\langle b\rangle^2/(10x) \qquad (10)$$

where x is the entanglement or cross-link spacing. It is surprising to see that good agreement is obtained in polymers as different as thermoplastics (PP) or thermosets (epoxies), taking into account the experimental scatter estimated for σ_i to $\sim 20\%$.

Effective stress and related activation parameters. There are three aspects to consider in this discussion: the degree of cross-linking, which is represented by the cross-link, or entanglement spacing x; the barrier height ΔG_0 of the local barrier, associated to cross-link points, which is represented by the athermal temperature T_a; and the chain flexibility, which is represented as the range of steric interactions of cross-link points by the length δ. *Table 5* gives T_a and *Table 6* gives δ and x in the case of epoxies and polyesters, while *Table 2* gives x and δ for the PP system. *Table 6* also gives structural parameters like M_e,

Table 5 Activation parameters for the crosslinked networks

Polymer	T_a (K)	ν_{def} (Hz)	α	ΔG_0 (eV)	$\mu(T_a, \nu_{def})$ (GPa)	$\sigma_i(T_a)$ exp (MPa)	σ_i/μ $\times 100$	$\mu\langle b\rangle/10x$ (MPa)
DGEBA-DDM	306	2×10^6	13.1	0.35	1.61	50	3.2	60
DGEBA-DDM/AN	316	2×10^6	13.1	0.35	1.61	38	2.4	44
DGEBA-HMDA	257	2×10^6	13.1	0.29	1.55	58	3.7	59
DGEBA-HMDA/HA	255	2×10^6	13.1	0.29	1.23	44	3.6	33
DGEBU-DDM	270	0.5×10^6	14.5	0.34	1.27	47	3.7	47
MAA-DEG	343	1×10^6	13.8	0.41	–	13	–	–
MAA-PG	380 433	3×10^6	12.7	0.42 0.47	– –	22 –	– –	– –

Table 6 Molecular parameters of the crosslinked networks. Symbols have the same meaning as in *Table 2*

Polymer	V_e (Å^3)	M_e (g mol^{-1})	δ (Å)	x (Å)	0.93δ (Å)	x^* (Å)	V_a (Å^3)	V_a/δ^2 (Å)
DGEBA-DDM	638.8	439	9.5	8.6	8.8	10.9	170	1.9
DGEBA-DDM/AN	1659	1116	9.5	11.8	8.8	14.9	165	1.8
DGEBA-HMDA	595.8	398	8	8.4	7.4	–	120	1.9
DGEBA-HMDA/HA	1696.8	1090	8	11.9	7.4	–	116	1.8
DGEBU-DDM	439.5	301	6.4	7.6	6	9.6	70	1.7
MAA-PG	275.5	195.9	(10.8)	6.5	(10)	8.2	–	–
MAA-DEG	307.5	220	–	6.7	–	8.5	–	–

the molecular weight, and V_e, the volume per cross-link point. The latter is computed from Van Krevelen[16] additive subgroup contributions, from which the parameter x is derived, $x^3 = V_e$. In order to simulate monoamine/diamine blends, of stoichiometry 60/40, V_e and M_e are computed from a statistical mixing of amine sequences: (i) N-DDM/N-ϕ/N-DDM and (ii) N-DDM/N-ϕ/N-ϕ/N-DDM (see *Table 3*), in which N-ϕ refers to aniline, as 0.4 (i) +0.6 (ii); similarly, for the unsaturated polyesters of concentration y in residual –CH=CH– groups, V_e and M_e are computed from the formula $yX^* + (1-y)X$, where X, X^* represent the quantity V_e or M_e taken in a saturated or in an unsaturated region of the network, respectively.

The most striking experimental feature in the epoxy system is that crosslinking affects only the internal stress σ_i and not the activation parameters like ΔG_0, α, T_a or V_a. This is clearly seen from *Tables 5* and *6* when comparing diamine with monoamine/diamine epoxies (e.g. DGEBA-DDM with DGEBA-DDM/AN); it is also quite visible on yield stress *versus* T curves[20] which run perfectly parallel (since V_a is proportional to their slopes). In contrast, the DGEBU-DDM curve shows a steeper slope (smaller V_a), but a comparable σ_i value. Therefore σ_i is merely a function of x, as has been proposed in equation (9), and obviously depends on the nature of the polymer by μ and $\langle b \rangle$.

The strength of local obstacles is measured by the athermal temperature $T_a = \Delta G_0/\alpha k$. Experiments on the epoxy system are of special interest since they show, as expected, that the local obstacles are in fact the cross-link points, here the –N–CH_2 groups. Examination of chemical structure in *Table 3* shows that, as far as –N–CH_2 groups are concerned, DGEBU-DDM and DGEBA-DDM have quite similar blocked configurations, while more mobility is expected from –$(CH_2)_6$– diamine sequences in DGEBA-HMDA. This order is modified when looking at hydroxyether groups, –CH(OH)–CH_2–O–, for which DGEBA-DDM and DGEBA-HMDA appear to be hindered, in contrast to the DGEBU-DDM resin in which the central methyl units –$(CH_2)_4$– may help them to move. Therefore, when looking at mechanical data for the relative strength of local obstacles in the three resins (since cross-link is not selective there), it is possible to decide which of the two molecular groups is relevant for the activation barrier. Barrier parameters in *Table 5*, T_a and ΔG_0, show conclusively that DGEBU and DGEBA-DDM resins behave in the same way, in favour of the cross-link nodes –N(CH_2)– being the obstacles. Moreover n.m.r. data[18], which follow mobility at 293–373 K by the $t^{1/2}$ method, give an entirely consistent classification, –N(CH_2)– groups being far more mobile in DGEBA-HMDA, and equivalent in the two other resins. Therefore, it is clear from this example that cross-link nodes, such as entanglements in thermoplastics, act as the local barrier to plastic deformation. The hydroxyether mobility, which is responsible for the β secondary transition, may also intervene in the mechanical behaviour but through another parameter, the molecular flexibility, represented by the length δ, and controlling the activation volume V_a, i.e. the T-slope of the yield stress (see below). It is worth noting that the classification of the three resins on their δ values (*Table 6*) is in complete agreement with n.m.r. data[18] on the hydroxether mobilities[17], the more mobile being here DGEBU-DDM ($\delta = 6.4$ Å), then DGEBA-HMDA ($\delta = 8$ Å), and the least mobile being DGEBA-DDM ($\delta = 9.5$ Å). The same order is seen for activation volumes. Hence the qualitative connection between chain flexibility and activation volume is confirmed by experiment.

The influence of molecular mobility on T_a is also exemplified in PP and PP blends. In PP blends T_a can be depressed by introducing some molecular mobility to the pure matrix, for example by diluting small quantities of PP-rich EPR copolymer chains within the diffuse interfacial zone around EPR particles. In such conditions, the activation entropy may be higher in the blend than in the pure homopolymer, resulting in a depression of T_a. This can be explained as follows. Porzucek has shown that the barrier enthalpy ΔH_0 of local obstacles is the same in PP and in PP blends[5,11], as expected when such obstacles are identified with chain entanglements. Since $\Delta H_0 = \Delta H_a(T_a)$, where the activation enthalpy, ΔH_a, behaves similarly to ΔG_0 in equation (4), $(\Delta G_0 + T_a \Delta S_0)_{PP} = (\Delta G_0 + T_a \Delta S_0)_{blend}$, it follows from equation (4) that:

$$T_a(\alpha k + \Delta S_0)_{PP} = T'_a(\alpha k + \Delta S'_0) \tag{11}$$

where T'_a and $\Delta S'_0$ refer to blend quantities (α is the same for pure PP and blends). As a consequence, $T_a > T'_a$ when $\Delta S_0 < \Delta S'_0$. Of course, the technological interest of depressing T_a is to depress the obstacle strength to plastic deformation, thus making the polymer tougher and more impact resistant.

Equation (11) has been solved for T'_a by Porzucek *et al.*[21]. Knowing $\Delta S_0 = \Delta S_a(T_a)$ from thermodynamic analysis[8], it becomes simply:

$$T_a(1 - zT_a) = T'_a(1 - z'T'_a) \tag{12}$$

where $z = (d\mu/\mu\, dT)$ and is determined by dynamic measurements. Therefore, from experimental determination of $z(T)$ and $z'(T)$ at the deformation frequency ν_{def}, T'_a can be deduced from T_a by graphic resolution, i.e. plotting the quantity $T(1-zT)$ *versus* T for PP and for the blend. For the EPR/HDPE/PP blend, with $T_a = 318$ K for PP, it gives $T'_a = 285$ K. Thus, the function $T(1-zT)$ shows most clearly the fine changes in molecular mobility that control yielding, while the usual $\tan\delta$ *versus* T plot would reveal hardly any significant difference between the homopolymer and its blend.

A last remark about T_a relates to its comparison with transition temperatures in molecular mobility determined at the deformation frequency ν_{def}. In general, no exact identification with peak temperatures should be expected, since T_a is related to the barrier energy ΔG_0 which is related only to some nucleation energy of β loops. However, the implied molecular motions are similar to those that occur in molecular transitions. Thus T'_a values fall near peak temperatures: 318 K in PP ($T_g = 311$ K), 343 K in MAA-DEG ($T_\beta = 340$ K), 380 and 433 K in MAA-PG ($T_\beta = 445$ K), 310–255 K in epoxies ($T_\beta = 360$–330 K). However, T_a values may sometimes be smaller than the peak temperature. This may occur since, even without mechanical help, the β dislocation loops are nucleated at the edge of the moving shear band front, where nucleation occurs more easily than outside.

The last structural ingredient for yield behaviour is the chain flexibility, which controls the activation volume. It is not easy to determine the range of hindrance caused by a cross-link node, δ, in thermoset networks, in which chains of unequal flexibility are issued from the same

node. However, it may be guessed as the largest spacing between the cross-link node and the nearest neighbouring rigid group along a chain. Accordingly, an n.m.r. picture of the various mobilities is necessary. In the case of DGEBA-HMDA, for example, n.m.r. shows a relatively mobile aliphatic sequence $-(CH_2)_6-$, a much less mobile hydroxyether group, and a rigid bisphenol A unit (see *Table 3*)[18]. Hence it seems reasonable to take δ as half the DGEBA unit length, i.e. $0.5L=\delta=8$ Å. Obviously, δ is not changed by the degree of cross-linking and is the same for HMDA-HA networks. Considering the two other epoxies, n.m.r. shows that the DGEBA unit behaves as a rigid rod up to the glass transition region. Therefore the two corresponding N-nodes are bound to each other, and might behave as a unique four-fold node, the spacing of which is given as $x^*=(2V_e)^{1/3}$ in *Table 6*. The length δ is then computed as the distance between the centre of DDM and the centre of DGEBA units, that is $\delta^2=(5.1)^2+(8)^2$, or $\delta=9.5$ Å for DGEBA-DDM resin. In the case of DGEBU-DDM, n.m.r. shows that the central methyls, $-(CH_2)_4-$, are easily moved so that δ is now taken from the centre of the DDM unit to the ether oxygen, –O–, of the DGEBA unit, that is $\delta^2=(5.1)^2+(3.9)^2$, or $\delta=6.4$ Å (the length of $-CH_2-CH(OH)-CH_2-O$ is the length of a cylindrical bead with the same radius as taken for the DGEBU unit in *Table 3*, i.e. 2.8 Å). Thus, as noted above, the corresponding order obtained in δ values for the three resins—DGEBA-DDM, DGEBA-HMDA and DGEBU-DDM—coincides with the order of hydroxyether mobility observed by n.m.r.[17,18], which gives at least a consistent experimental check to the determination of δ values.

Knowledge of the parameter δ for each resin allows the activation volume to be predicted by comparing it with the cross-link spacing x or x^*, depending on the case. Thus it is seen from *Table 6* that all five epoxy resins investigated fulfil the relation $x>0.93\delta$ (or $x^*>0.93\delta$); that is to say that all these resins are examples of case 1 (see above) of independent obstacles, and should fulfil equation (7) for the activation volume, as do the simple thermoplastics of *Table 2*. In order to check this prediction, *Table 6* lists values of $f\beta=V_a/\delta^2$ for the epoxies. It is very interesting to see that the low temperature V_a value, which is observed to be constant[6] over about 80°C, fits very well with the prediction of the model with $f\beta\cong 1.8\pm 0.1$ Å, the same value as for the thermoplastics listed in *Table 2*. Considering the experimental scatters (5–10% on V_a) and the very different polymers investigated, this agreement gives a sound basis to the proposed yield model.

Looking now at unsaturated polyesters, n.m.r. and dynamic mechanical analysis report no other β mobility than that due to 'network defects', as recalled earlier, i.e. at unsaturated $-CH=CH-$ bonds. As in DDM resins, the two cross-link nodes (here $-\underset{|}{CH}-$) at each extremity of rigid MAA–styrene–MAA blocks behave as paired mates, with a spacing $x^*=(2V_e)^{1/3}$ given in *Table 6*. Along the same lines as above, δ may tentatively be attributed only to nodes near an unsaturated bond. In the case of MAA-DEG, the distance between the midpoint of a styrene branch and the neighbouring $-CH=CH-$ group, that is $\delta^2=(2.3)^2+(10.6)^2$, gives $\delta=10.6$ Å. Nevertheless this value is probably only a lower bound, owing to the fact that β mobility is concerned only on one arm of the cross-link node, the others belonging to saturated regions

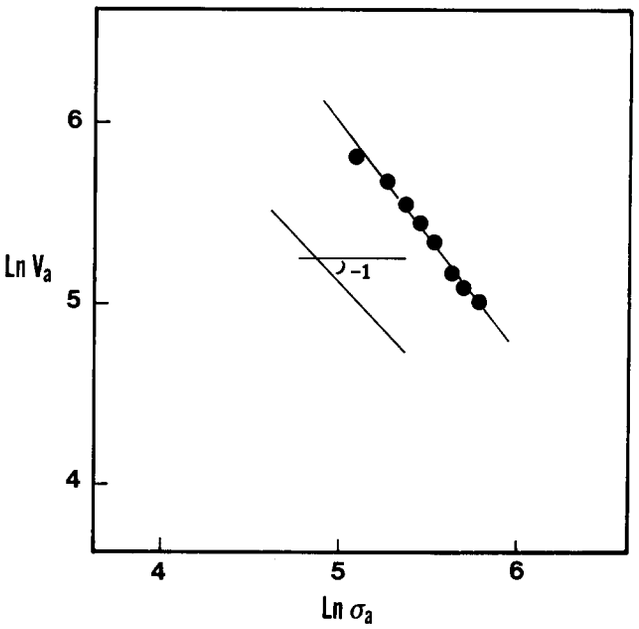

Figure 3 Stress dependence of the activation volume (log–log plot) in MAA-PG networks. (V_a is in Å^3 and σ_a is in MPa)

of the polyester network. For this reason, this value is given in parentheses in *Table 6*. Even with this estimation it is seen that $x^*<0.93\delta$, and the same would apply to MAA-PG. Therefore, in contrast to epoxies, the unsaturated polyesters in this study fall in case (2) of overlapping obstacles, or Peierls forces case. Again, in agreement with observations the low temperature activation volume at yield is no longer constant, but should vary noticeably with the yield stress[7], approximately as $(\sigma_a-\sigma_i)^{-1}$ as predicted by equation (8). This is verified in the log–log plot of *Figure 3* in the case of MAA-PG networks (V_0 is plotted as a function of σ_a but it nevertheless provides a reasonable test of equation (8) since μ and therefore σ_i are only weakly temperature dependent in that range). As both polyester networks, MAA-DEG and MAA-PG, have the same parameters ($\langle b\rangle\cong 4.8$ Å, as in PS, due to lateral phenyl rings in the styrene links; $x\cong 6.6$ Å) identical values of the activation volume are expected, and are observed in conformity with predictions.

To sum up, obstacles of both regimes have been observed, and the fairly good agreement between theory and experiment in the two cases confirms that the activation volume is controlled by local chain flexibility.

ACKNOWLEDGEMENTS

This work was made possible through the financial support of DRET for the model epoxy networks, Norsolor/ORKEM for the unsaturated polyesters and Atochem for the polypropylene blends. Dr B. Bloch of ONERA, Paris, prepared the model epoxies. Dr A. Piras of Norsolor/ORKEM, Centre de Recherches de Verneuil, prepared the polyesters.

REFERENCES

1 Escaig, B. *Helvet. Phys. Acta* 1983, **56**, 293
2 Escaig, B. *Polym. Eng. Sci.* 1984, **24**, 737
3 Escaig, B. in 'Dislocations in Solids', Yamada Conference (Ed. H. Suzuki), University of Tokyo Press, Tokyo, 1985, p. 559
4 Lefebvre, J. M. Thèse de Doctorat d'Etat, Université de Lille, 1982

5 Porzucek, K. Thèse de Doctorat de l'Université de Lille, 1988
6 Fernagut, F. Thèse de Doctorat de l'Université de Lille, 1990
7 Melot, D. Thèse de Doctorat de l'Université de Lille, 1989
8 Escaig, B. in 'Plastic Deformation of Amorphous and Semi-crystalline Materials' (Eds B. Escaig and C. G'Sell), Les Editions de Physique, les Ulis, 1982, p. 187
9 Escaig, B. and Lefebvre, J. M. *Rev. Phys. Appl.* 1978, **13**, 285
10 Friedel, J. in 'Alliages et Métaux Amorphes', 21ème colloque de Métallurgie INSTN, CEN-Saclay, Gif-sur-Yvette, 1978, p. 59
11 Porzucek, K., Lefebvre, J. M., Coulon, G. and Escaig, B. J. *Mater. Sci.* 1989, **24**, 3154
12 Fitzpatrick. J. R. and Ellis, B. in 'The Physics of Glassy Polymers' (Ed. R. N. Haward), Applied Science Publishers, London, 1973, pp. 142, 144
13 Kirste, R. G. and Oberthur, R. C. in 'Small Angle X-ray Scattering' (Eds O. Glatter and O. Kratky), Academic Press, London, 1982, pp. 427, 428
14 Dipersio, J. Thèse de Doctorat d'Etat, Université de Lille, 1980
15 Porzucek, K., Lefebvre, J. M., Coulon, G. and Escaig, B. *J. Mater. Sci.* 1989, **24**, 2533
16 Van Krevelen, D. W. and Hoftyser, P. J. 'Properties of Polymers', Elsevier, Amsterdam, 1976, pp. 590–596
17 Cukierman, S., Eustache, R. P., Halary, J. L., Lauprêtre, F. and Monnerie, L. Contrat DRET 87/140, Final report, Paris, 1990
18 Eustache, R. P. Thèse de Doctorat de l'Université Paris 6, 1990
19 Lefebvre, J. M. and Escaig, B. *J. Mater. Sci.* 1985, **20**, 438
20 Caux, X., Coulon, G. and Escaig, B. *Polymer* 1988, **29**, 808
21 Porzucek, K., Lefebvre, J. M. and Escaig, B. *J. Mater. Sci. Lett.* 1989, **8**, 1445